

# PHYSICAL REVIEW B

## CONDENSED MATTER

THIRD SERIES, VOLUME 49, NUMBER 17

1 MAY 1994-I

### Effects of sample preparation on the stopping powers of Havar for protons and $\alpha$ particles

L. E. Porter

*Department of Physics, Washington State University, Pullman, Washington 99164-2814*

E. Rauhala and J. Räsänen

*Department of Physics, University of Helsinki, SF-00170 Helsinki, Finland*

(Received 23 April 1993; revised manuscript received 6 January 1994)

The stopping powers of Havar for 0.5–2.4 MeV protons and 1.2–1.8 MeV  $\alpha$  particles have been measured with uncertainties of a little more than 0.6% and slightly less than 0.6%, respectively. Havar foils with three different tempers—cold-rolled, annealed, and heat-treated—were used in order to learn if stopping power might be influenced by type of target foil preparation. The results indicated no such influence, since all measurements were mutually consistent. Moreover, these data were thoroughly amenable to analysis with modified Bethe-Bloch theory, which yielded generally plausible values of the parameters appearing in the modified Bethe-Bloch formula. Recommended values of these parameters are  $I=299.3\pm 3.3$  eV for the mean excitation energy, and  $b=1.33\pm 0.04$  with  $\xi=1.0$  for the two Barkas-effect parameters.

#### I. INTRODUCTION

Havar is an alloy<sup>1</sup> widely used for containment of various gas targets for accelerated ion beams. Hence it is often necessary to know with great accuracy the energy loss of projectiles traversing these foils. Calculation of energy loss over a broad interval of projectile velocity can be performed with modified Bethe-Bloch theory.<sup>2</sup> This theory, however, applies directly to targets of isolated atoms of the same species. When bonding effects arise, as in the cases of condensed states and of compounds or alloys, a first approximation is to employ the additivity rule<sup>3</sup> for stopping effects. Higher accuracy can be obtained only from a resort to experiment.

One of the earliest measurements,<sup>4</sup> performed with deuteron projectiles at Wisconsin, indicated an unexpectedly large departure from the additivity assumption<sup>5</sup>. Subsequent measurements with light projectiles by one of the authors (L.P.) at Los Alamos<sup>6</sup> and by another experimental group at Auckland<sup>7</sup> provided results quite consistent with additivity predictions,<sup>6</sup> however. Yet another measurement,<sup>8</sup> with proton projectiles at Neuchatel, showed remarkable consistency with the original Wisconsin data,<sup>4,5</sup> and at least four subsequent sets of measurements<sup>9–12</sup> at Helsinki by two of the authors (E.R. and J.R.) have shown mixed results, according to a recent survey and analysis of extant data by the other author (L.P.).<sup>13</sup>

Dispersion among various sets of stopping power measurements has long been a source of concern, if not dismay.<sup>14</sup> Whereas it is sometimes feasible to select, on

some rational basis, a set or sets of measurements as preferred, such is not always the case. The aforementioned survey revealed that essentially every set of Havar measurements provided an excellent fit to modified Bethe-Bloch theory, but that the stopping powers themselves differed considerably and, of course, so did the parameters of the theory extracted from analyses.<sup>13</sup> Inconsistencies exist even among separate sets of measurements by the same author(s), as is the case for Refs. 5 and 6 and for Refs. 9–12. In an attempt to furnish an explanation for the observed discrepancies, it was conjectured that the method of target foil preparation during the manufacturing process might somehow be responsible.<sup>13</sup> An experiment to test his hypothesis had already been initiated at the time of the reported survey.<sup>13</sup>

The goal was to measure stopping powers for light projectiles with Havar foils from at least two different preparation processes.<sup>13</sup> In this spirit foils with three separate, documented histories of preparation process were procured, and measurements with proton and  $\alpha$  particle projectiles were initiated.

#### II. THEORY AND METHOD OF ANALYSIS

The stopping power  $S$  of a target of atomic number  $Z$  and atomic weight  $A$  for a projectile of atomic number  $z$  and velocity  $v=\beta c$  can be calculated<sup>14</sup> in units of keV cm<sup>2</sup>/mg as

$$S = \frac{0.30708z^2Z}{\beta^2 A} L, \quad (1)$$

where  $L$  is the complicated, but dimensionless, stopping number per target electron. The latter quantity can be written as the sum of three terms,

$$L = L_0 + \xi z L_1 + L_2. \quad (2)$$

Here  $L_0$  is the basic stopping number,

$$L_0 = \ln \frac{2mc^2 \beta^2}{1 - \beta^2} - \beta^2 - \ln I - C/Z - \delta/2, \quad (3)$$

where  $mc^2$  denotes the rest mass energy of the electron,  $I$  represents the mean excitation energy,  $C$  stands for total shell corrections, and  $\delta$  is the density effect correction for highly relativistic projectiles.<sup>15</sup> The second term of  $L$  constitutes the Barkas-effect correction term  $zL_1$  prefaced by an amplitude  $\xi$  for use in data fits. The third term of  $L$ ,  $L_2$ , denotes the Bloch term<sup>16</sup> only recently restored to the stopping-power formula.<sup>17</sup> This term can be evaluated as

$$L_2 = \psi(1) - \text{Re}[\psi(1 + iy)], \quad (4)$$

where  $\psi$  is the digamma function<sup>18</sup> and  $y = z\alpha/\beta$  with  $\alpha$  signifying the fine-structure constant.

A further modification of Bethe-Bloch stopping-power theory must be invoked when the projectile has slowed to a velocity comparable to those of target atomic electrons. In this case some version of projectile effective charge must be defined and included in the formalism.<sup>2,19</sup> In this study the projectile velocity intervals were such as to preclude use of such a correction factor, save possibly at the very lowest one or two energies. Hence the complicating effective charge factor was neglected.

Some discretion in choice of various parameters of the theory can be exercised. The shell corrections free of distortions from association with higher-order  $z$  effects are those selected for analysis, i.e., the  $K$ - and  $L$ -shell corrections calculated by Walske<sup>20</sup> and adapted to more general cases by Bichsel,<sup>21</sup> as described by Berger and Seltzer.<sup>22</sup> In this rubric the total of shell corrections is given by

$$C = C_K(\beta^2) + V_L C_L(H_L \beta^2) + V_M C_L(H_M \beta^2) + V_N C_L(H_N \beta^2), \quad (5)$$

where the  $C_K$  and  $C_L$  signify the Walske  $K$ - and  $L$ -shell corrections,<sup>20</sup> respectively, and the  $V_i$  and  $H_i$  ( $i = L, M, N$ ) denote the scaling factors.<sup>21,22</sup> The mean excitation energy of a given target can rarely be calculated from first principles, and hence is often obtained from interpolation, extrapolation, or fits to experimental data. The Barkas-effect correction term can be calculated from one of at least three extant formalisms.<sup>23-28</sup> These methods have been compared in a recent review,<sup>29</sup> with the result that the first published<sup>23-26</sup> proved most effective in providing accurate fits for light projectiles penetrating a wide range of elemental target materials.<sup>29</sup> Thus the first method<sup>23-26</sup> has been adopted, providing for calculation of  $L_1$  from the expression,

$$L_1 = \frac{F(b/x^{1/2})}{Z^{1/2} x^{3/2}}, \quad (6)$$

where  $F$  denotes a function graphed in Ref. 23,  $b$  is the

only free (composite) parameter of the formalism,<sup>23-26</sup> and  $x = (18787)\beta^2/Z$ . The value of  $b$  can be obtained in the same manner as that described for  $I$ . All of the description of Bohr and Bethe theory presupposes a target consisting of identical atoms completely separated from each other, since this model is the basis of descriptions of energy-loss processes.<sup>30</sup> If atoms are in the condensed phase, or combined into molecules, or both, "aggregation effects" require that compensations be made. An extended treatment of aggregation effects may be found in Refs. 13 and 31, where application of Bragg's rule of additivity<sup>3</sup> is discussed in detail. The parameter generally selected for testing additivity is the mean excitation energy, whose (Bragg rule) average value is given<sup>30,31</sup> by

$$\ln I_B = \frac{\sum_j n_j Z_j \ln I_j}{\sum_j n_j Z_j}, \quad (7)$$

where  $n_j$ ,  $Z_j$ , and  $I_j$  represent the atomic concentration, atomic number, and mean excitation energy of the  $j$ th component of the composite material. The preceding version of modified Bethe-Bloch theory was utilized in the current study to extract various target parameter values from fits to the measurements.

### III. EXPERIMENT AND RESULTS

Target foils of three different types of preparation and in the two nominal thicknesses of 2.4 and 4  $\mu\text{m}$  were procured from the supplier<sup>1</sup> in an attempt to test the aforementioned hypothesis concerning the observed dispersion among various sets of stopping-power measurements. After consultation with the technical office<sup>32</sup> of the supplier, it was decided to utilize foils obtained in three different tempers: cold-rolled, annealed, and heat-treated. The areal densities of the foils were determined by weighing a circular (20-mm diameter) piece from each foil. Two different microbalances were used in order to test for consistency. The foil areas were determined with a microscope. The areal densities thus obtained for cold-rolled, annealed, and heat-treated foils were, for the thinner set, 1.966 mg/cm<sup>2</sup>, 1.778 mg/cm<sup>2</sup>, and 1.845 mg/cm<sup>2</sup>, respectively, and for the thicker set, 3.415 mg/cm<sup>2</sup>, 3.104 mg/cm<sup>2</sup>, and 3.570 mg/cm<sup>2</sup>, respectively.

The  $^1\text{H}^+$  and  $^4\text{He}^+$  beams were produced by the 2.5-MV Van de Graaff accelerator at the University of Helsinki. The energy calibration of the beam-analyzing magnet was based on the resonances at 991.9 and 1799.8 keV in the reaction  $^{27}\text{Al}(p, \gamma)^{28}\text{Si}$ . Standard scattering equipment as described in Ref. 33 was used. The experimental arrangement is presented in more detail in Ref. 9. Collimating slits and apertures were used to limit the beam spot size on the target to 0.5 mm in diameter and the beam angular divergence to 0.04°. A silicon surface barrier detector (50 mm<sup>2</sup>, 100  $\mu\text{m}$ ), with a detection solid angle of 0.30 mSr, was positioned at a scattering angle of 135°. The energy resolution of the detecting system was 12 keV. The detection system featured a linear energy dependence, so that a constant value of particle energy per channel was observed.

In the energy-loss measurement backscattered ions from a thick gold target, or, alternatively, from thin gold films on a silicon substrate, were employed. The scattered flux of ions then penetrated through the foil placed perpendicular to the scattered beam in front of the detector. Thus direct beam exposure, which could modify the properties of the foils, was avoided. In addition, the possibility of contamination of the target by the accelerator beam was eliminated. The most probable energy loss of the ions in the foils was then determined for the transmission geometry by observing the shift of the backscattering signal induced by the foil. (Previous studies of spectra obtained in similar measurements with the same experimental apparatus indicated that the displacement between the desired average energy loss and the most probable energy loss was negligible.)

The stopping power at the mean ion energy ( $E_{av}$ ) in the foil was calculated by dividing the energy loss ( $\Delta E$ ) by the foil areal density ( $\rho\Delta x$ ) ( $\rho$  represents mass density,  $\Delta x$  is the foil thickness, and  $E_{av} = E_i - \Delta E/2$ , where  $E_i$  = incident energy). To account for the nonlinear dependence on ion energy of stopping powers, a small correction to the mean energy ( $E_{av}$ ) was applied. As a result, the stopping power,  $S = -(1/\rho)(dE/dx)$  (differential energy loss per unit path length), is taken as  $\Delta E/\rho\Delta x$  at an effective ion energy,  $E_{eff}$ . The correction procedure for obtaining  $E_{eff}$  from  $E_{av}$  is valid only when  $\Delta E < E_{av}$ . Several independent sets of measurements were carried out in this experiment, which was confined to the energy intervals of 0.5–2.4 MeV and 1.2–1.8 MeV for protons and  $\alpha$  particles, respectively.

The estimated errors in the energy loss values are 0.3 and 0.4 % for  $\alpha$  particles and protons, respectively. An accuracy of 0.5% in the areal densities was estimated. This value arises from the possible uncertainty in the

weighing procedures and the nonuniformity of the foils. The uniformity of each foil was checked by energy-loss measurements from ten different spots on the foil. The average energy loss thus obtained was then used for normalizing the other data. In this way we could confirm that the weighed areal density obtained corresponded to the effective local area density used in the energy-loss experiments.

Experimental results are summarized in tables of measured stopping powers. Table I contains results for protons of various projectile energies traversing the cold-rolled, annealed, and heat-treated foils. Similarly, Table II contains results for  $\alpha$  particles of various projectile energies traversing cold-rolled, annealed, and heat-treated foils. When these data were graphed to enable comparison of results for the three different types of sample preparation for the same projectile, it became quite clear that there was no significant systematic difference among the three data sets. In order to demonstrate even more clearly the observed consistency among the three sets of measurements, fits were made with modified Bethe-Bloch stopping power theory so as to compare among three sets of extracted parameter values. Quality of fit was appraised, as always, on the basis of the root-mean-square relative deviation of calculated from measured stopping-power values  $\sigma$ .

#### IV. ANALYSIS AND RESULTS

The modified Bethe-Bloch formalism that can be used to analyze data was set forth in Sec. II above. The several target-dependent parameters appearing therein were the mean excitation energy ( $I$ ), the shell corrections ( $C$ ), and the two parameters associated with the Barkas-effect formalism<sup>23–26</sup> selected ( $b$  and  $\xi$ ). The roles of the

TABLE I. Measured stopping powers( $S$ ) of cold-rolled, annealed, and heat-treated Havar foils for proton projectiles at listed average (corrected) energies ( $E$ ).

Cold-rolled		Annealed		Heat-treated	
$E$ (MeV)	$S$ (MeV cm <sup>2</sup> /g)	$E$ (MeV)	$S$ (MeV cm <sup>2</sup> /g)	$E$ (MeV)	$S$ (MeV cm <sup>2</sup> /g)
0.5617	174.9	0.5822	171.2	0.5748	172.7
0.7076	157.1	0.7388	153.7	0.6935	157.7
0.7089	156.3	0.7399	153.1	0.6946	157.2
0.7097	155.9	0.7401	153.0	0.6947	157.1
0.7101	155.7	0.7406	152.9	0.6960	156.4
0.7104	155.9	0.7413	152.2	0.6968	156.6
0.8445	139.3	0.8590	137.8	0.8534	138.9
1.0062	128.5	1.0290	126.9	0.9964	128.4
1.1093	120.4	1.1222	118.7	1.1170	120.1
1.2812	112.1	1.2998	111.4	1.2747	110.9
1.3692	106.3	1.3798	105.6	1.3757	106.2
1.3694	106.0	1.3800	105.3	1.3759	106.0
1.5485	99.7	1.5647	99.3	1.5420	99.2
1.6261	95.0	1.6351	94.9	1.6318	95.1
1.8103	90.5	1.8244	90.4	1.8039	90.2
1.8792	87.5	1.8880	86.8	1.8841	87.9
2.0864	83.4	2.0814	83.2	2.0625	83.1
2.1308	81.5	2.1387	81.2	2.1353	81.9
2.3237	77.8	2.3364	77.3	2.3187	77.3
2.3820	76.0	2.3890	76.1	2.3867	75.8

TABLE II. Measured stopping powers ( $S$ ) of cold-rolled annealed, and heat-treated Havar foils for  $\alpha$  particle projectiles at listed average (corrected) energies ( $E$ ).

Cold-rolled		Annealed		Heat-treated	
$E$ (MeV)	$S$ (MeV cm <sup>2</sup> /g)	$E$ (MeV)	$S$ (MeV cm <sup>2</sup> /g)	$E$ (MeV)	$S$ (MeV cm <sup>2</sup> /g)
1.1970	805.2	1.2945	802.9	1.2593	804.3
1.3620	791.4	1.4617	779.3	1.4232	787.2
1.3649	789.0	1.4622	778.8	1.4233	787.1
1.3693	785.1	1.4630	778.0	1.4245	786.0
1.3711	783.5	1.4638	777.3	1.4251	785.5
1.3713	783.4	1.4645	776.5	1.4257	784.9
1.5226	775.5	1.6180	767.4	1.5827	771.8
1.7422	749.5	1.8320	739.8	1.7994	744.4
1.7431	748.7	1.8322	739.5	1.7995	744.3
1.7447	747.3	1.8344	737.3	1.8011	742.7
1.7448	747.2	1.8362	735.5	1.8016	742.2
1.7449	747.0	1.8377	734.0	1.8031	740.8
1.7562	740.5	1.8438	730.2	1.8086	738.7

latter two parameters in an analysis of measurements are discussed in Ref. 13. Target shell corrections feature several parameters that could serve as searched parameters in an analysis. However, the shell corrections represent a relatively small fraction of the total stopping number, so that a fit of measurements would show little sensitivity to appreciable changes in the values of these parameters. Hence these quantities are most often calculated from a rubric devised by Bichsel,<sup>21</sup> subsequently described by Berger and Seltzer,<sup>22</sup> and exempted from inclusion in searches during analyses of measurements. The target mean excitation energy is by far the dominant parameter appearing in the stopping number. Thus in almost every analysis of data this parameter serves as a searched quantity. (An exception is the case of determining values of charge-state parameters<sup>2,19,34</sup>.)

In this study the parameters whose values were sought are the mean excitation energy and the Barkas-effect parameters. Measurements will generally support the extraction of two parameters and those of sufficient accuracy and density will support the extraction of three. The current measurements fall in the latter category. Thus two-parameter searches were conducted for  $I$  and  $b$  with  $\xi$  fixed, and for  $I$  and  $\xi$  with  $b$  fixed. Shell correction scaling parameters were assigned the values obtained from an application of the Bichsel prescription.<sup>21,22</sup>  $V_L = 1.00$ ,  $H_L = 1.00$ ,  $V_M = 1.875$ ,  $H_M = 7.13$ . A Bragg-rule value of mean excitation energy  $I_B$  was calculated from Eq. (7), utilizing the constituent mean excitation energies<sup>22,35</sup> displayed in Table III, for use as a comparison

standard for extracted values of this parameter. The value thus obtained was  $I_B = 295.8$  eV.

The first set of two-parameter fits was conducted for proton projectiles with  $\xi$  fixed at 1 in order to extract best-fit values of  $I$  and  $b$ . Results are shown in Table IV. The pairs of values of  $I$  and  $b$  thus determined for each type of target foil manifested remarkable consistency to confirm the aforementioned finding that stopping powers appeared not to depend on target foil preparation. Moreover, the average values of  $I$  and  $b$ , 299.3 eV and 1.33, respectively, agreed very well with the expected values<sup>13</sup> of  $I_B = 295.8$  eV and  $b = 1.36$ , respectively. Similarly, when the value of  $b$  was fixed at 1.36, the extracted values of  $I$  and  $\xi$  evinced the same sort of consistency, as expected, with average extracted values of  $I$  and  $\xi$  at 301.4 eV and 1.09, respectively.

The fitting procedure utilized for  $\alpha$  particle projectiles was the same as that used for proton projectiles. Results are displayed in Table V. When  $\xi$  was set at 1, extracted  $I$  values were closely bunched about the average value of 291.1 eV, whereas  $b$  remained at 1.60 for all three foils. The latter value lay slightly above the expected range<sup>26</sup> of  $1.4 \pm 0.1$ . Indeed, the resulting average values of  $I$  and  $\xi$ , with  $b$  fixed at the lower value of 1.36, strayed downward to 284.1 eV and (a constant) 0.60, respectively.

The data thus provided best-fit values of parameters that were both internally consistent and close to expected values for all the cases of two-parameter fits. Hence the analysis was extended to three-parameter fits, with  $I$  and the (interdependent) Barkas-term parameters as the

TABLE III. Values of selected constituent mean excitation energies for Havar.

Element	$I$ (eV)	Ref.	Element	$I$ (eV)	Ref.
H	20.4	35	Mn	272	22
Be	63.7	22	Fe	286	22
C	78.0	22	Co	297	22
N	82.0	22	Ni	311	22
O	95.0	22	Mo	424	22
Cr	257	22	W	727	22

TABLE IV. Results of two-parameter fits for protons traversing cold-rolled, annealed, and heat-treated Havar foils.

Foil type	Fixed parameter	$I$ (eV)	$b$	$\sigma$
Cold-rolled	$\xi=1.0$	298.8	1.33	1.22
Annealed	$\xi=1.0$	299.0	1.33	1.40
Heat-treated	$\xi=1.0$	300.1	1.34	0.78
			$\xi$	
Cold-rolled	$b=1.36$	300.4	1.08	1.23
Annealed	$b=1.36$	299.8	1.06	1.40
Heat-treated	$b=1.36$	304.0	1.12	0.78

searched quantities. The results of this enterprise, shown in Table VI, were again most plausible. Best-fit average values of  $I$  were 297.5 eV and 295.1 eV for proton and  $\alpha$  particle projectiles, respectively. Corresponding average values of  $b$  and  $\xi$ , 1.22 and 0.82, respectively, lay slightly below expected values for the Ritchie-Brandt suggestion<sup>26</sup> of  $1.4\pm 0.1$  and 1, respectively, for the case of protons. By contrast, corresponding average (constant) values of  $b$  and  $\xi$ , 2.11 and 2.34, respectively, lay somewhat above expected values for the Lindhard suggestion<sup>17</sup> of  $1.8\pm 0.2$  and 2, respectively, for the case of  $\alpha$  particles. Quality of fit was considerably better in the case of  $\alpha$  particle projectiles.

The stopping-power measurements for foils of different preparations were consistent within experimental uncertainties, as noted above. Moreover, extracted parameters of modified Bethe-Bloch theory yielded values consistent among the three types of foil, as expected. Since there were no significant differences among the three sets of data, a single set for each projectile type was selected for graphic display. For both two- and three-parameter fits, the foil type chosen was that which provided the best quality of fit for both types of projectile, namely, the heat-treated type. In the case of two-parameter fits, the calculated curve for both projectiles was that with  $\xi$  set at 1.0. These cases yielded  $I$  values that were quite consistent—300.1 and 290.1 eV, respectively. Furthermore, the  $I$  values yielded by these foils in the three-parameter fits were 294.2 and 298.3 eV for protons and  $\alpha$  particles, respectively. These  $I$  values lay between the two values obtained in the two-parameter fits, so that all four evinced a reasonable measure of internal consistency.

A further question that naturally arises pertains to the

TABLE V. Results of two-parameter fits for  $\alpha$  particles traversing cold-rolled, annealed, and heat-treated Havar foils.

Foil type	Fixed parameter	$I$ (eV)	$b$	$\sigma$
Cold-rolled	$\xi=1.0$	292.3	1.60	1.36
Annealed	$\xi=1.0$	290.8	1.60	1.18
Heat-treated	$\xi=1.0$	290.1	1.60	1.07
			$\xi$	
Cold-rolled	$b=1.36$	285.6	0.60	1.91
Annealed	$b=1.36$	283.6	0.60	1.47
Heat-treated	$b=1.36$	283.1	0.60	1.50

TABLE VI. Results of three-parameter fits for protons and  $\alpha$  particles traversing cold-rolled, annealed, and heat-treated Havar foils.

Foil type	$I$ (eV)	$b$	$\xi$	$\sigma$
Proton projectiles				
Cold-rolled	297.2	1.18	0.78	1.20
Annealed	296.9	1.22	0.82	1.38
Heat-treated	298.3	1.25	0.85	0.74
$\alpha$ particle projectiles				
Cold-rolled	295.9	2.11	2.34	0.76
Annealed	295.1	2.11	2.34	0.71
Heat-treated	294.2	2.11	2.27	0.38

size of the uncertainties in parameter values extracted from measurements. A method of response to this question was devised and described previously.<sup>2,34</sup> The results of applying this technique to the heat-treated foil measurements and extracted parameter values for two-parameter fits are summarized in Table VII. (The fixed values of  $b$  and  $\xi$  utilized for the  $\alpha$  particle cases correspond to the Lindhard suggestion.<sup>17</sup>) The uncertainty values attest further to the remarkable consistency of measurements among the three types of foil investigated. The sizes of uncertainties displayed are surely characteristic for the cases where specific calculations were not made. (The method of calculation is quite time consuming, so that only typical values are generally computed.<sup>2,34</sup>)

Graphs of the stopping powers of heat-treated foils for protons and  $\alpha$  particles are provided in Figs. 1 and 2, respectively, including the curves obtained from two-parameter and three-parameter fits as described above. The prediction of another currently used computer code,<sup>36,37</sup> TRIM-92, is shown for comparison in each figure. The excellence of fit to these data with modified Bethe-Bloch theory, for eminently plausible values of the free parameters therein, is readily apparent

## V. SUMMARY

A set of measurements of the stopping powers of Havar for protons and  $\alpha$  particles has been added to the world sample. Both the data and the parameter values extracted therefrom manifest remarkable internal consistency. A prominent outcome of this investigation is the refutation of the hypothesis of one author (L.P.) that stopping powers of Havar foils might depend on the

TABLE VII. Parameter values and calculated uncertainties for two-parameter fits of both proton and  $\alpha$  particle data obtained with heat-treated foils.

Projectile	$I\pm\Delta I$ (eV)	$b+\Delta b$	$\xi+\Delta\xi$
Protons	$304.0\pm 3.3$	[1.36 fixed]	$1.12\pm 0.06$
Protons	$300.1\pm 2.8$	$1.34\pm 0.04$	[1.00 fixed]
$\alpha$ particles	$290.0\pm 0.4$	[1.80 fixed]	$1.40\pm 0.01$
$\alpha$ particles	$294.5\pm 0.6$	$2.00\pm 0.01$	[2.00 fixed]

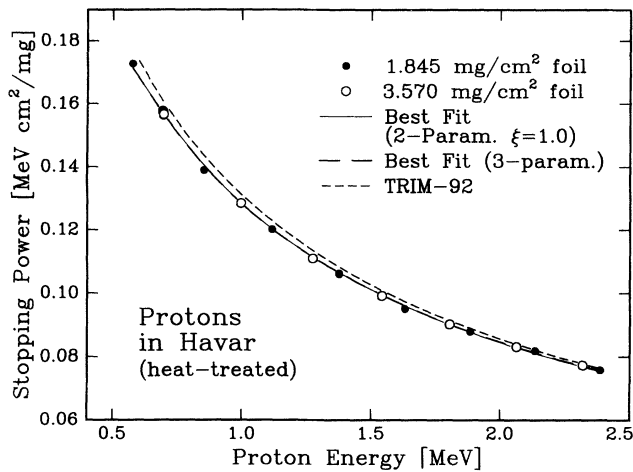


FIG. 1. The experimental stopping powers of heat-treated foils for protons and the curves obtained from two- and three-parameter fits. The predictions obtained by the TRIM-92 computer code are shown for comparison. The two- and three-parameter best fits overlap.

method of preparation. Another noteworthy feature of these measurements is the larger mean excitation energy extracted from proton data compared to that extracted from  $\alpha$  particle data in every type of fit, although the trend is more evident for two-parameter fits than for three-parameter fits. This feature, observed not only for Havar and Mylar foils<sup>13</sup> but for some inert gas targets as well,<sup>38</sup> might raise doubt as to the correctness of the projectile- $z$  dependence of stopping power contained in modified Bethe-Bloch theory. However, the trend was not observed in the case of Al, Cu, and Ag foils.<sup>34</sup>

Recommended parameter values were selected from among the various sets of values obtained in fits. Some preference was given the proton data set on the basis of the considerably broader energy interval from which it was collected. Insofar as guideline values are concerned, the additivity-based Bragg value of mean excitation energy served as such, as did either set of recommended ( $b, \xi$ ) values, i.e., the Ritchie-Brandt<sup>26</sup> set of  $(1.4 \pm 0.1, 1)$  or the Lindhard<sup>17</sup> set of  $(1.8 \pm 0.2, 2)$ . More specifically, in the

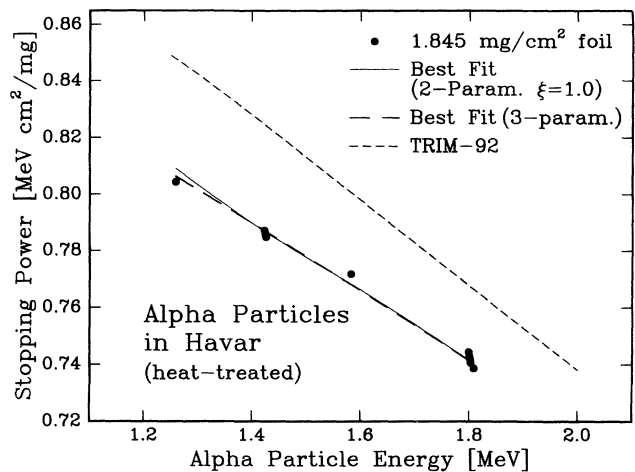


FIG. 2. The experimental stopping powers of the heat-treated thin foil for  $\alpha$  particles and the curves obtained from two- and three-parameter fits. The predictions obtained by the TRIM-92 computer code are shown for comparison.

case of the Ritchie-Brandt set<sup>26</sup> one might expect  $b = 1.36$  or so on the basis of previous studies.<sup>2,13,39</sup> One generally expects small deviations from the Bragg value of  $I$  in the case of medium- $Z$  alloys,<sup>31</sup> although very few tests have been conducted for such materials.<sup>40</sup> In view of these considerations, recommended values of  $I$ ,  $b$ , and  $\xi$  are  $299.3 \pm 3.3$  eV,  $1.33 \pm 0.04$ , and 1, respectively. The  $I$  value exceeds the Bragg value by slightly more than 1%, which lies within the uncertainty assigned to  $I$ , or, for that matter, within the uncertainty that could be assigned to  $I_B$  because of uncertainties in constituent  $I$  values.

#### ACKNOWLEDGMENTS

The authors are especially grateful to Hamilton Precision Metals of Lancaster, PA, and to Martin Bradley, Senior Process Metallurgist, in particular, for providing the Havar foil samples utilized in this experiment.

<sup>1</sup>Havar is a cobalt-based alloy supplied by Hamilton Precision Metals of Lancaster, PA, 17604-3014.

<sup>2</sup>See, e.g., L. E. Porter, *Radiat. Res.* **110**, 1 (1987).

<sup>3</sup>W. H. Bragg and R. Kleeman, *Philos. Mag.* **10**, 318 (1905).

<sup>4</sup>L. E. Porter and L. C. McIntyre (unpublished).

<sup>5</sup>L. E. Porter, L. C. McIntyre, and W. Haerberli, *Nucl. Instrum. Methods* **89**, 237 (1970).

<sup>6</sup>C. L. Shepard and L. E. Porter, *Phys. Rev. B* **12**, 1649 (1975).

<sup>7</sup>J. C. Duder, J. F. Clare, and H. Naylor, *Nucl. Instrum. Methods* **123**, 89 (1975).

<sup>8</sup>F. Foroughi, B. Vuilleumier, and E. Bovet, *Nucl. Instrum. Methods* **159**, 513 (1979).

<sup>9</sup>E. Rauhala and J. Räsänen, *Nucl. Instrum. Methods Phys. Res. Sect. B* **12**, 321 (1985).

<sup>10</sup>E. Rauhala and J. Räsänen, *Nucl. Instrum. Methods Phys. Res. Sect. B* **24/25**, 362 (1987).

<sup>11</sup>E. Rauhala and J. Räsänen, *Nucl. Instrum. Methods Phys. Res. Sect. B* **35**, 130 (1988).

<sup>12</sup>A. Z. Kiss, E. Somorjai, J. Räsänen, and E. Rauhala, *Nucl. Instrum. Methods Phys. Res. Sect. B* **39**, 15 (1989).

<sup>13</sup>L. E. Porter, *Radiat. Eff. Defects Solids* **117**, 197 (1991).

<sup>14</sup>See, e.g., H. Bichsel and L. E. Porter, *Phys. Rev. A* **25**, 2499 (1982).

<sup>15</sup>R. M. Sternheimer, M. J. Berger, and S. M. Seltzer, *At. Data Nucl. Data Tables* **30**, 261 (1984).

<sup>16</sup>F. Bloch, *Ann. Phys. (Leipzig)* **16**, 285 (1933).

<sup>17</sup>J. Lindhard, *Nucl. Instrum. Methods* **131**, 1 (1976).

<sup>18</sup>*Handbook of Mathematical Functions*, edited by M.

- Abramowitz and I. A. Stegun (National Bureau of Standards, Washington, DC, 1964), p. 259.
- <sup>19</sup>L. E. Porter, Nucl. Instrum. Methods Phys. Res. Sect. B **12**, 50 (1985).
- <sup>20</sup>M. C. Walske, Phys. Rev. **88**, 1283 (1952); **101**, 940 (1956).
- <sup>21</sup>H. Bichsel (private communication).
- <sup>22</sup>M. J. Berger and S. M. Seltzer, *Stopping Power and Ranges of Electrons and Positrons*, NBSIR 82-2550-A (National Bureau of Standards, Washington, DC, 1983).
- <sup>23</sup>J. C. Ashley, R. H. Ritchie, and W. Brandt, Phys. Rev. B **5**, 2393 (1972).
- <sup>24</sup>J. C. Ashley, R. H. Ritchie, and W. Brandt, Phys. Rev. A **8**, 2402 (1973).
- <sup>25</sup>J. C. Ashley, Phys. Rev. B **9**, 334 (1974).
- <sup>26</sup>R. H. Ritchie and W. Brandt, Phys. Rev. A **17**, 2102 (1978).
- <sup>27</sup>D. L. Jackson and R. L. McCarthy, Phys. Rev. B **6**, 4131 (1972).
- <sup>28</sup>S. H. Morgan and C. C. Sung, Phys. Rev. A **20**, 818 (1979).
- <sup>29</sup>L. E. Porter and Hong Lin, J. Appl. Phys. **67**, 6613 (1990).
- <sup>30</sup>U. Fano, Ann. Rev. Nucl. Sci. **13**, 1 (1963).
- <sup>31</sup>W. H. Barkas and M. J. Berger, in *Penetration of Charged Particles in Matter*, National Academy of Sciences—National Research Council Publication No. 1133 (NAS-NRC, Washington, DC, 1967).
- <sup>32</sup>Martin Bradley (private communication).
- <sup>33</sup>A. Fontell and M. Luomajärvi, Phys. Rev. B **19**, 159 (1979).
- <sup>34</sup>L. E. Porter and S. R. Bryan, Radiat. Res. **97**, 25 (1984).
- <sup>35</sup>J. F. Janni, At. Data Nucl. Data Tables **27**, 147 (1982); **27**, 341 (1982).
- <sup>36</sup>J. F. Ziegler, J. P. Biersack, and V. Littmark, *The Stopping and Ranges of Ions in Matter* (Plenum, New York, 1985), Vol. 1.
- <sup>37</sup>J. F. Ziegler and J. P. Biersack, TRIM-92 computer code (private communication).
- <sup>38</sup>L. E. Porter, Nucl. Instrum. Methods Phys. Res. Sect. B **69**, 39 (1992).
- <sup>39</sup>L. E. Porter, Phys. Rev. B **40**, 8530 (1989).
- <sup>40</sup>D. I. Thwaites, Radiat. Res. **95**, 495 (1983).